CrystEngComm

PAPER

View Article Online
View Journal | View Issue

Cite this: *CrystEngComm*, 2014, **16**, 6450

Synthon polymorphs of 1 : 1 co-crystal of 5-fluorouracil and 4-hydroxybenzoic acid: their relative stability and solvent polarity dependence of grinding outcomes†

Song Li,[ab] Jia-Mei Chen*[a] and Tong-Bu Lu*[ac]

Received 28th January 2014,
Accepted 9th April 2014

DOI: 10.1039/c4ce00221k

www.rsc.org/crystengcomm

Although polymorphism is a common phenomenon, the polymorphism of co-crystals is not studied extensively as compared to single-component molecules. Herein we report polymorphism in a co-crystal system comprising 5-fluorouracil, and 4-hydroxybenzoic acid with a 1 : 1 stoichiometry. The polymorphs were characterized by single-crystal and powder X-ray diffraction, differential scanning calorimetry and thermogravimetric analysis. Crystal structure analysis revealed different synthons of 5-fluorouracil and 4-hydroxybenzoic acid in two forms. The solvent-drop grinding experiments show a high degree of solvent polarity specificity. The theoretical and experimental methods suggest an enantiotropic relationship between the polymorphs.

Introduction

Polymorphism is the ability of a solid material to be crystallized in at least two crystal structures.[1] This phenomenon is common in drugs, agrochemicals, pigments, dyes and explosives, *etc.*[2–5] Polymorphism has gained considerable interest since different polymorphs exhibit different physical and chemical properties such as melting point, solubility, chemical stability, moisture sorption tendency, compressibility, and processability.[6–11] The origin of polymorphism can be classified into four categories: packing polymorphism, conformational polymorphism, tautomeric polymorphism, and synthon polymorphism. Packing polymorphism refers to identical molecular moieties packing into different periodic crystal structures.[12–14] Conformational polymorphism is defined as molecular moieties with rotational degrees of freedom which adopt different conformations in the crystal.[14,15] Tautomeric polymorphism appears when tautomers crystallize from the solution, in which the tautomers coexist and equilibrate at the crystallization temperature.[16–18] Synthon polymorphism occurs when the primary synthons in the forms are different.[14,19]

Polymorphism has been studied widely in single-component molecules but its occurrence in multi-component systems such as co-crystals has not been extensively addressed.[20–42] A co-crystal is built up by at least two components that are solids under ambient conditions coexisting through non-covalent interactions.[43] The study of co-crystals is currently of interest since they are exploited to yield new crystalline forms of materials with desirable physical and chemical properties.[44–49]

Herein we report supramolecular synthon polymorphism in a 1 : 1 co-crystal of 5-fluorouracil (5FU) and 4-hydroxybenzoic acid (4HBA) (see Scheme 1). 5FU, a chemotherapeutic agent, is a pyrimidine analogue with multiple N–H donors and C=O acceptors and exhibits the diversity of hydrogen bonding motifs from a crystal engineering viewpoint.[50] 4HBA is one of the most commonly used co-formers for co-crystallization of

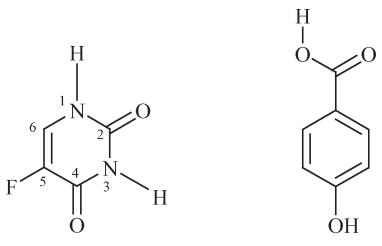

5FU **4HBA**

Scheme 1 Structures of 5-fluorouracil (5FU) and 4-hydroxybenzoic acid (4HBA).

[a] *School of Pharmaceutical Sciences, Sun Yat-Sen University, Guangzhou 510006, China. E-mail: chenjm37@mail.sysu.edu.cn, lutongbu@mail.sysu.edu.cn; Fax: +86 20 84112921*
[b] *School of Life Sciences, Sun Yat-Sen University, Guangzhou 510275, China*
[c] *MOE Key Laboratory of Bioinorganic and Synthetic Chemistry, School of Chemistry and Chemical Engineering, Sun Yat-Sen University, Guangzhou 510275, China*

† Electronic supplementary information (ESI) available: IR spectra, DSC and TG curves of **Form I** and **Form II**, PXRD date with regard to grinding experiments and slurry experiments, VT-PXRD of **Form II**, CCDC 983683 and 983684 for **Form II** and **Form I**, respectively. For ESI and crystallographic data in CIF or other electronic format see DOI: 10.1039/c4ce00221k

active pharmaceutical ingredients because of its carboxyl and hydroxyl functional groups as well as its low toxicity.[51–53] We now reveal two polymorphs of the title co-crystal and report our observations dealing with phase transformations and relative stability of the forms. The two polymorphs were characterized by various analytical techniques, such as single-crystal and powder X-ray diffraction, differential scanning calorimetry, and thermogravimetric analysis.

Experimental

Reagents

5FU (**Form I**) was purchased from Melon Pharmaceutical Co., Ltd, and 4HBA was purchased from Aladdin reagent Inc. They were used without any further purification. All other reagents and solvents obtained from commercial suppliers were used as received.

Preparation of polymorphs

Form I was prepared *via* the following two methods: (i) a mixture of 5FU (130 mg, 1 mmol) and 4HBA (138 mg, 1 mmol) was added to 1 mL of water and allowed to stir at 50 °C or room temperature (RT) for 24 h. The suspension was filtered and the isolated solid of **Form I** was dried under vacuum for 24 h. Yield: 220.8 mg, 82.4%. The filtrate was left to evaporate slowly at RT. After two weeks, rod-shaped crystals of **Form I** were obtained. Anal. (%) calcd for $C_{11}H_9FN_2O_5$: C, 49.26; H, 3.38; N, 10.45. Found: C, 49.28; H, 3.40; N, 10.41. IR (KBr, $\nu_{C=O}$): 1710 (s), 1649 (s) cm^{-1}. (ii) A 1 : 1 mixture of 5FU (130 mg, 1 mmol) and 4HBA (138 mg, 1 mmol) was added to a stainless steel grinding jar. Approximately two drops of water was added, and the mixture was ground for 30 min at a frequency of 25 Hz.

Form II was obtained *via* the following two methods: (i) a mixture of 5FU (130 mg, 1 mmol) and 4HBA (138 mg, 1 mmol) was dissolved in 2 mL of water with stirring at 65 °C, then the resulting solution was filtered immediately. Upon rapid cooling to RT and standing for 24 h, block-shaped crystals of **Form II** were harvested. Yield: 201.5 mg, 75.2%. Anal. (%) calcd for $C_{11}H_9FN_2O_5$: C, 49.26; H, 3.38; N, 10.45. Found: C, 49.24; H, 3.36; N, 10.43. IR (KBr, $\nu_{C=O}$): 1715 (s), 1676 (s) cm^{-1}. (ii) A 1 : 1 mixture of 5FU (130 mg, 1 mmol) and 4HBA (138 mg, 1 mmol) was added to stainless steel grinding jar. Approximately two drops of THF was added, and the mixture was ground for 30 min at a frequency of 25 Hz.

Grinding experiments

Grinding was performed using a Retsch Mixer Mill model MM200 with two 25 ml stainless steel grinding jars and two 15 mm stainless steel grinding balls at a rate of 25 Hz for 30 min. All the experiments were carried out with a 1 : 1 stoichiometric ratio of 5FU (130 mg, 1 mmol) and 4HBA (138 mg, 1 mmol). For solvent-drop grinding experiments, two drops of a selected solvent with different dielectric constant were added to the reactants prior to grinding. The resulting solids were analyzed by PXRD to identify the polymorph.

Slurry experiments

Excess amounts (approximately 100 mg) of **Form I** and **Form II** in a 1 : 1 ratio were added to 1 mL of aqueous solution, which was saturated with 5FU (0.09 mmol) and 4HBA (0.05 mmol) in advance. The resulting slurries were allowed to stir at ambient conditions for 1 day. The solids were collected by vacuum filtration and analyzed by PXRD.

Single-crystal X-ray diffraction (SXRD)

SXRD data of **Form I** and **Form II** were collected at 150 K on an Agilent Xcalibur Nova CCD diffractometer, with graphite monochromated Cu Kα radiation (λ = 1.5418 Å). Cell refinement and data reduction were applied using the program package CrysAlis PRO. The structures were solved by direct methods and refined by the full-matrix least-squares method on F^2. All the non-hydrogen atoms were refined anisotropically. All hydrogen atoms were refined at geometrically constrained riding positions. All the calculations were performed using the SHELX-97 program. The crystallographic data are summarized in Table 1, and selected hydrogen bonding distances and angles are given in Table 2.

Powder X-ray diffraction (PXRD)

Room temperature PXRD analysis was performed on a Bruker D2 Advanced diffractometer (Bruker, PHASER) operated with Cu Kα radiation (λ = 1.5418 Å) at 30 kV and 10 mA. The data were collected over an angular range of 5°–40° (2θ) value in continuous scan mode using a step size of 0.014° (2θ) and a step time of 0.1 s. Typically, 30 mg of solid was used for analysis and pressed gently on a silicon slide to give a level surface. Variable temperature PXRD (VT-PXRD) data were obtained on a Bruker D8 Advance with Cu Kα radiation (40 kV, 40 mA). Each sample was scanned between 5° and 40° (2θ) with 0.02° (2θ) step size and 0.12 s per step scan speed. Calculated PXRD patterns were generated from the single-crystal structure data using Mercury CSD 3.1 (Cambridge crystallographic data center, UK).

Infrared (IR) spectroscopy

IR (KBr pellet) spectra were recorded on a Bruker EQUINOX 55 FT-IR spectrometer. A total of 64 scans were collected over a range of 4000 to 400 cm^{-1} with a resolution of 0.2 cm^{-1} for each sample.

Differential scanning calorimetry (DSC)

DSC was recorded in a nitrogen atmosphere using a Netzsch DSC-204 Instrument. The sample was placed in an aluminium pan and scanned from 30 °C to a final temperature of 180 °C at a heating rate of 10 °C min^{-1}.

Table 1 Crystallographic data and refinement parameters for **Form I** and **Form II**

	Form I	**Form II**
Formula	$C_{11}H_9FN_2O_5$	$C_{11}H_9FN_2O_5$
M_r	268.20	268.20
Temperature/K	150.02(11)	150.00(10)
Crystal size/mm^3	0.20 × 0.1 × 0.1	0.20 × 0.20 × 0.10
Wavelength/Å	1.5418	1.5418
Crystal system	Monoclinic	Triclinic
Space group	$P2_1/c$	$P\bar{1}$
a/Å	7.0356(3)	6.8225(6)
b/Å	14.9022(13)	8.6115(9)
c/Å	10.2665(4)	10.7203(12)
α (°)	90	67.906(10)
β (°)	99.418(4)	86.057(8)
γ (°)	90	78.308(8)
V_{cell}/Å^3	1061.90(11)	571.46(10)
Z	4	2
ρ(calcd)/g cm^{-3}	1.678	1.559
μ/mm^{-1}	1.265	1.176
F(000)	552	276
θ range (°)	5.28–62.95	4.45–62.94
Index ranges	−7, 7; −17, 16; −10, 11	−7, 5; −9, 9; −10, 12
Reflections collected	3520	3293
Independent reflections	1690 [R(int) = 0.0413]	1808 [R(int) = 0.0329]
Completeness	98.5%	98.1%
Data/restraints/parameters	1690/0/185	1808/0/182
GOF	1.055	1.054
Final R indices [$I > 2\sigma(I)$][a]	R_1 = 0.0617, wR_2 = 0.1490	R_1 = 0.0456, wR_2 = 0.1106
R indices (all data)[a]	R_1 = 0.1014, wR_2 = 0.1844	R_1 = 0.0630, wR_2 = 0.1266
Largest diff. peak, hole (e Å^{-3})	0.269, −0.436	0.208, −0.275

[a] $R_1 = \sum||F_o| - F_c||/\sum|F_o|$. w$R_2 = [\sum[w(F_o^2 - F_c^2)^2]/\sum w(F_o^2)^2]^{1/2}$, $w = 1/[\sigma^2(F_o)^2 + (aP)^2 + bP]$, where $P = [(F_o^2) + 2F_c^2]/3$.

Table 2 The hydrogen bonding distances and angles for **Form I** and **Form II**

Compound	H bond	D–H/Å[g]	H···A/Å[g]	D···A/Å[g]	∠D–H···A/Å[g]
Form I	O(4)–H(4)···O(2)[a]	0.82	1.84	2.640(5)	164.4
	N(1)–H(1)···O(1)[b]	0.82(5)	2.21(5)	3.028(4)	172(5)
	N(2)–H(2)···O(5)[c]	0.89(4)	1.90(4)	2.784(6)	168(3)
	O(3)–H(3)···O(1)	0.86(7)	2.17(7)	3.019(5)	167(6)
Form II	N(2)–H(2)···O(2)[d]	0.93(3)	1.94(3)	2.847(2)	164(2)
	N(1)–H(1)···O(2)[e]	0.92(3)	1.89(3)	2.805(2)	176(2)
	O(4)–H(4)···O(5)[f]	0.82	1.80	2.615(2)	176.1
	O(3)–H(3)···O(1)	0.82	1.94	2.645(2)	144.3

[a] Symmetry codes: [x, y + 1, z]. [b] [−x + 1, −y + 1, −z + 2]. [c] [−x + 1, −y, −z]. [d] [−x + 2, −y + 1, −z + 2]. [e] [−x + 1, −y + 1, −z + 2]. [f] [−x + 1, −y, −z]. [g] D and A are hydrogen bond donors and acceptors.

Thermogravimetric analysis (TGA)

TGA was performed using a Netzsch TG-209 instrument. The sample was placed in an aluminium sample pan and heated over the temperature range of 30–500 °C at a heating rate of 10 °C min^{-1}.

Stability test

The stability of **Form I** and **Form II** was evaluated at 40 °C/75% relative humidity (RH). A vial of each sample was subjected to the conditions for one month. Then the samples were immediately analyzed by PXRD.

Results and discussion

To evaluate the potential for co-crystallization behavior of 5FU and 4HBA as co-formers, the structures of pure 5FU and 4HBA were analyzed from a crystal engineering perspective. **Form I** of 5FU (refcode FURACL14) adopts a hydrogen-bonded sheet structure exploiting all of the available uracil donors and acceptors (including double hydrogen bond homosynthon A, Scheme 3) and exhibiting regions where the fluorine atoms are in close proximity, approaching within 3.2 Å (Scheme 2). The crystal structure of 4HBA (refcode JOZZIH) shows that two 4HBA molecules form a dimer through the acid–acid

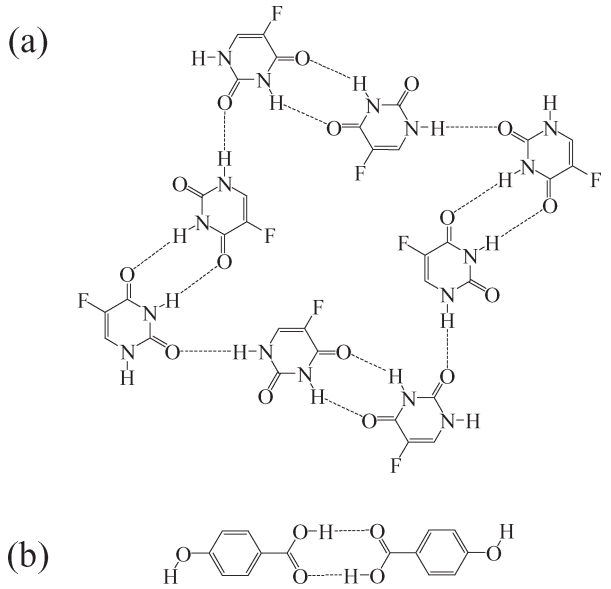

Scheme 2 Hydrogen-bonded sheet structure of **Form I** of 5FU (a) and acid–acid dimer structure of 4HBA (b).

$R_2^2(8)$[54] doubly hydrogen bonded homosynthon D (Schemes 2 and 3). When 5FU co-crystallizes with 4HBA, all their hydrogen bond donors and acceptors adjust to achieve a balance of all parts of the two molecules. Some supramolecular homosynthons motifs in pure 5FU and 4HBA must be interrupted, whereas some new heterosynthons must be generated.

Crystal structures of Form I and Form II

The crystal structure of **Form I** belongs to the monoclinic, $P2_1/c$ space group (Table 1). The asymmetric unit contains one 5FU molecule and one 4HBA molecule (Fig. 1a). Two 5FU molecules are connected through a doubly hydrogen bonded $R_2^2(8)$ homosynthon (synthon A) to form a dimer, and two 5FU-dimers are further connected with two 4HBA molecules through two amide–acid $R_2^2(8)$ heterosynthons (synthon E) and two O3–H3···O1 hydrogen bonds (synthon F) to form a one-dimensional (1D) chain (Fig. 1b). The 1D chains are packed to form a two-dimensional (2D) sheet *via* F···F (2.850 Å) interactions[55] and van der Waals force (Fig. 1b). The 2D sheets further stack along the *c*-axis through the interlayer π···π interactions (3.58 Å) between the rings of 5FU and 4HBA to form the three-dimensional (3D) structure (Fig. 1c, d). In **Form I**, each 5FU molecule generates two hydrogen bonds with adjacent 5FU molecules and three hydrogen bonds with adjacent 4HBA molecules, and each 4HBA molecule forms three hydrogen bonds with two adjacent 5FU molecules (Fig. 1b).

The crystal structure of **Form II** was solved in a triclinic, $P\bar{1}$ space group (Table 1). The asymmetric unit also contains one 5FU molecule and one 4HBA molecule (Fig. 2a). 5FU molecules are connected through two doubly hydrogen bonded $R_2^2(8)$ homosynthons (synthon B and C) to generate a 1D chain. 4HBA molecule links another 4HBA molecule through an acid–acid $R_2^2(8)$ homosynthon (synthon D) to form a carboxylic dimer. The 5FU 1D chains are further connected by 4HBA dimers through O3–H3···O1 hydrogen bonds (synthon F) to generate a 2D sheet (Fig. 2b). The 2D sheets are packed along the *b*-axis *via* interlayer π···π interactions (3.49 Å) between the rings of 5FU and 4HBA to form the 3D structure (Fig. 2c, d). In **Form II**, each 5FU molecule forms four hydrogen bonds with adjacent 5FU molecules and one hydrogen bond with adjacent 4HBA molecules, and each 4HBA molecule generates one hydrogen bond with adjacent 5FU molecules and two hydrogen bonds with adjacent 4HBA molecules (Fig. 2b).

From the crystal structure analysis, we can see that these two forms are synthon polymorphs since their primary synthons are different. The acid–acid homosynthon (synthon D) of 4HBA

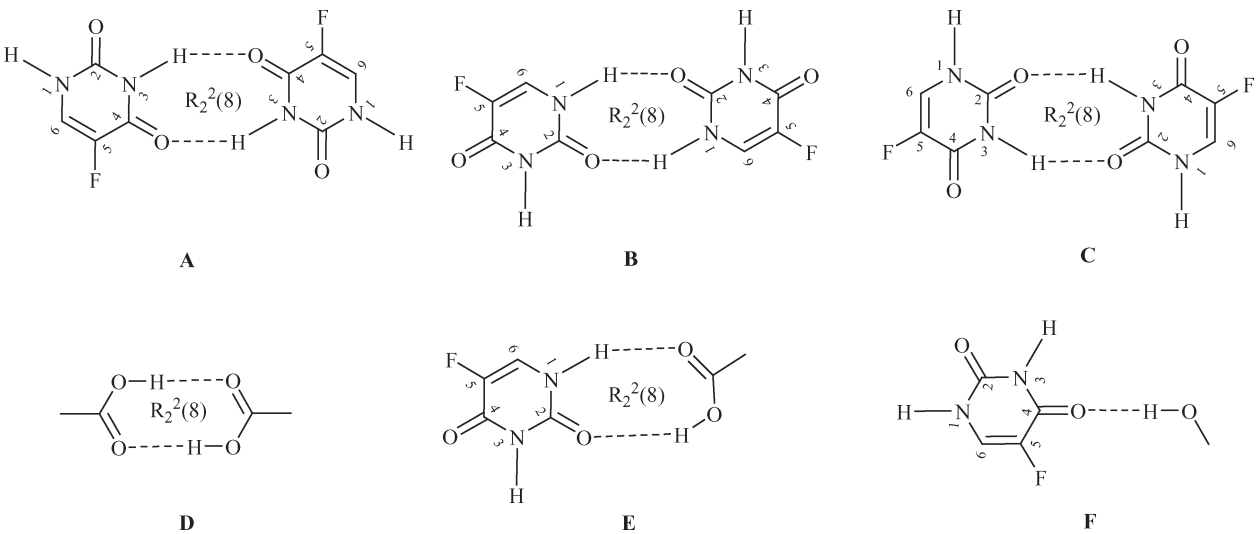

Scheme 3 Homo- and heterosynthons exhibited by 5FU-4HBA co-crystal polymorphs.

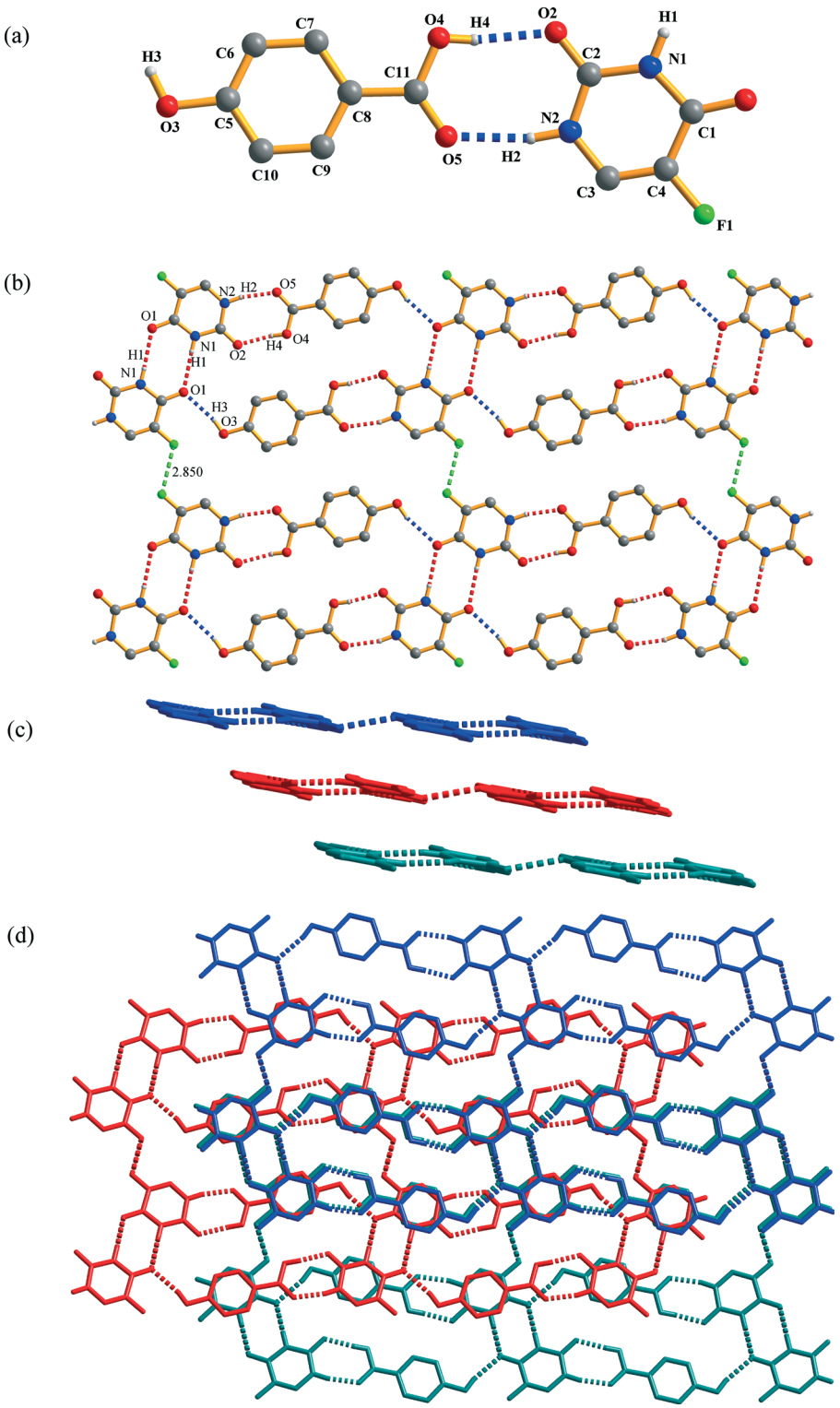

Fig. 1 (a) The molecular structure, (b) 2D sheet, (c) side view and (d) top view of 3D structure (the blue, red and teal color are the first, second and third layer, respectively) of **Form I**.

is interrupted and new heterosynthons (synthons E and F) are generated in **Form I**, while synthon D of 4HBA is preserved and only heterosynthon F is generated in **Form II**. As a result, all hydrogen-bonding sites in 5FU and 4HBA molecules are effectively utilized in **Form I** and **Form II**.

PXRD and thermal analyses

The PXRD patterns of the bulk batch of **Form I** and **Form II** are different from either that of 5FU or 4HBA (Fig. 3a and b), indicating the formation of new crystalline phases. In addition, all the peaks displayed in the measured patterns closely

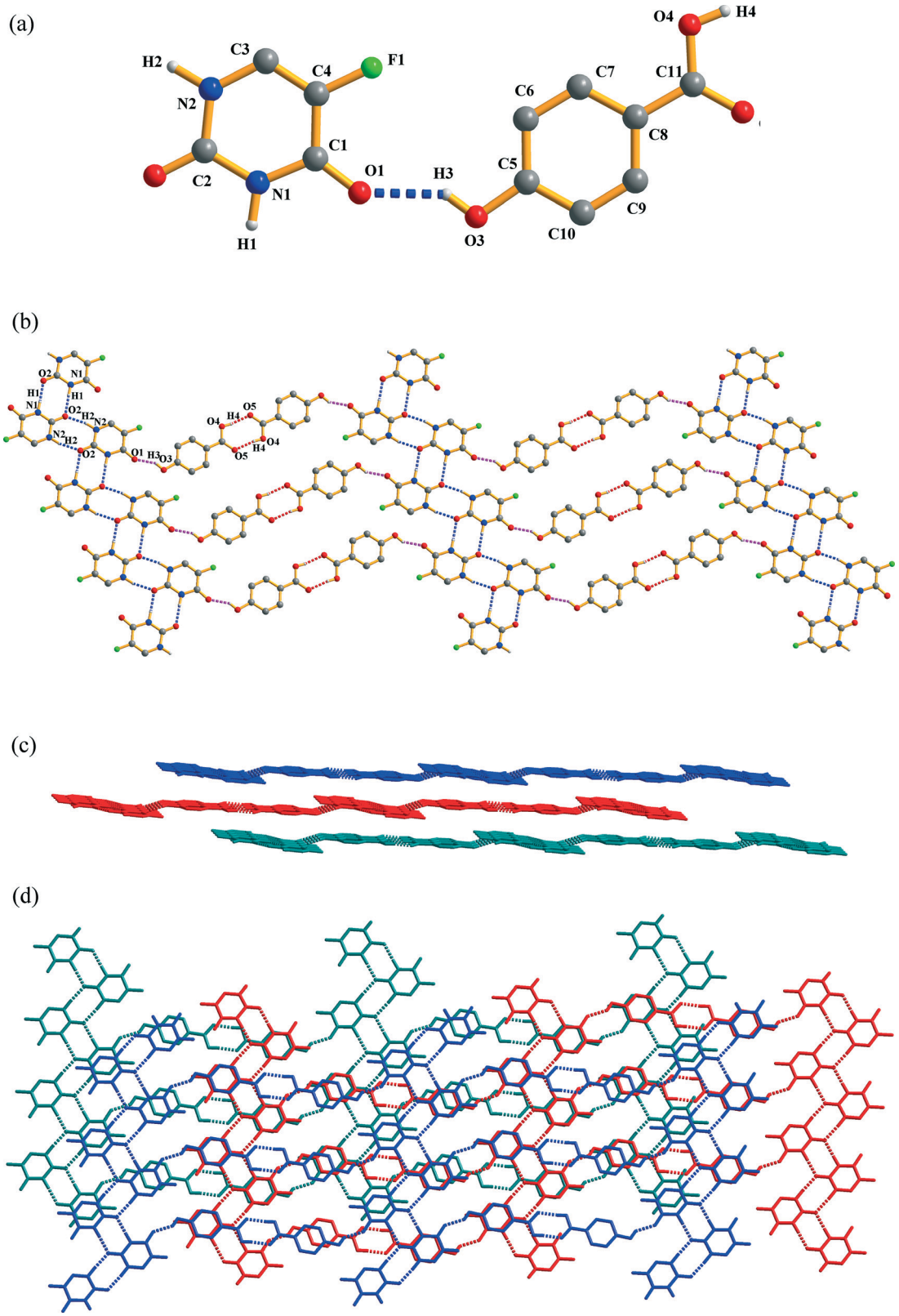

Fig. 2 (a) The molecular structure, (b) 2D sheet, (c) side view and (d) top view of 3D structure (the blue, red and teal colors are the first, second and third layers, respectively) of **Form II**.

match those in the simulated patterns generated from single-crystal diffraction data (Fig. 3a and b), confirming the formation of the corresponding polymorphic forms. The displacement of the peaks at the high angle regions between the measured

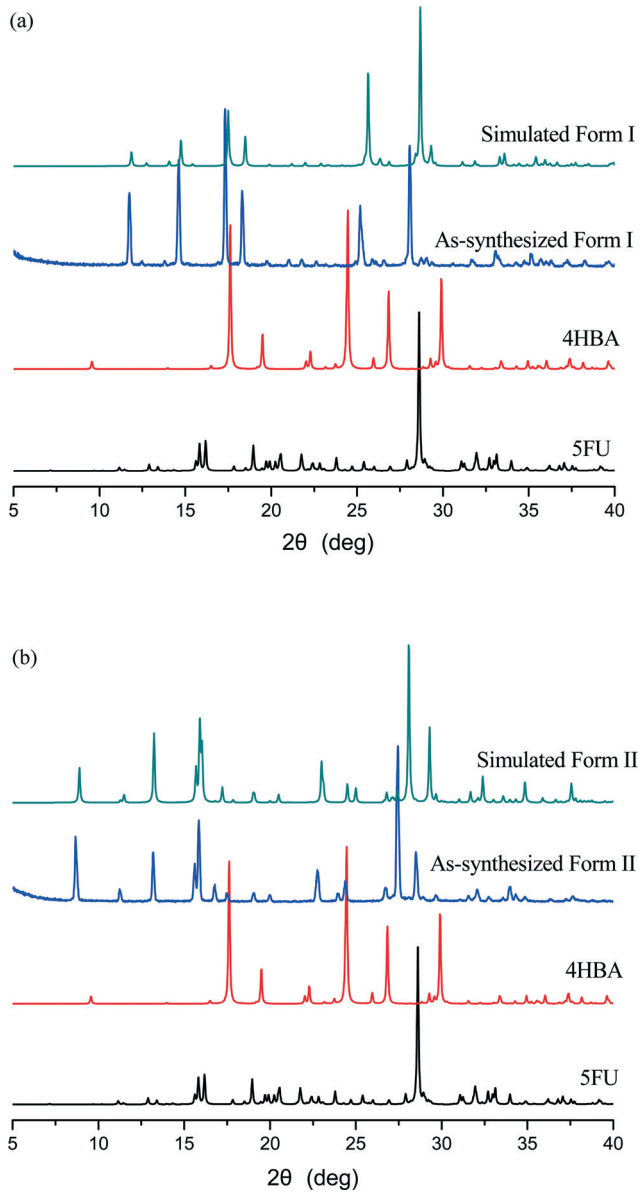

Fig. 3 PXRD patterns of 5FU, 4HBA, as-synthesized by the solution crystallization method, and simulated from the single-crystal data for (a) **Form I** and (b) **Form II**.

and simulated patterns is mainly caused by the different measuring temperature between the powder patterns (room temperature) and the single-crystal data (150 K).

From the DSC and TGA curves it can be found that both **Form I** and **Form II** decompose on heating (about 179 °C) before melting. There is no evidence of a phase transformation in a DSC curve of either form before decomposition (Fig. S2†).

Solid-state grinding experiments

Solid-state grinding is a green approach for co-crystal screening, which can avoid excessive use of crystallization solvent.[56,57] This method can also offer a high yield of co-crystal, without any waste by being dissolved in solutions. Solid-state grinding can be classified into two categories: solvent-drop grinding (SDG) and neat grinding (NG), which differ in adding or not adding solvent when grinding.[58,59]

NG and SDG were conducted using a 1 : 1 molar ratio of 5FU and 4HBA. The resulting solids were analyzed by PXRD to identify the crystal form. Dry grinding of 5FU with 4HBA for 30 minutes resulted in generation of **Form II**. SDG was performed using each of the solvents selected with different dielectric constants (Table 3). The results of the SDG experiment revealed that **Form II** was produced when low polar solvents were used. As the polarity of solvent increased, a mixture of **Form I** and **Form II** was generated. Pure **Form I** can be obtained when the polarity of solvents increases further (Fig. S3†). These observations suggest a high degree of solvent polarity specificity for the grinding experiments. Low polar solvents have a higher tendency to generate **Form II**, while high polar solvents tend to generate **Form I**. Similar polarity dependent polymorphic outcomes of grinding experiments have been reported before.[61–64]

A kinetically reasoned hypothesis can account for the different outcome of grinding experiments with high polar solvents (**Form I**) and low polar solvents (**Form II**). In the presence of high polar solvents, the carboxyl group of 4HBA, the highest polar group in two molecules, is tightly solvated, resulting in the disruption of the doubly hydrogen-bonded acid–acid dimers (synthon D) in 4HBA during grinding. In contrast, this group is much less strongly solvated in low polar solvents and leaves synthon D in 4HBA intact during grinding. Thus the strong solvation of the carboxyl group of 4HBA with high polar solvents provides a barrier to the preservation of the acid–acid $R_2^2(8)$ motif in **Form I**, suggesting such kinetic effects may play a major role in determining the polymorphic outcome.

Relative stability of Form I and Form II

Relative polymorph stabilities can usually be determined by theoretical and experimental approaches. From a theoretical aspect, typically, the higher the density of a polymorph the higher its stability.[65] The calculated density of **Form I** (1.678 g cm^{-3}) is higher than that of **Form II** (1.559 g cm^{-3}), indicating that **Form I** will be the stable form at low temperatures.

From an experimental aspect, a slurry experiment, also referred to as a solvent-mediated phase transformation experiment, was conducted to estimate the relative thermodynamic stability of **Form I** and **Form II** at RT. A powdered 1 : 1 mixture of these two forms was stirred in water for 24 h. Then the resulting solid was filtered off, dried under vacuum and measured by PXRD. The results of the PXRD analysis revealed that the mixture completely converted to **Form I**, suggesting that **Form I** is more stable than **Form II** in aqueous solution at RT (Fig. S4†). Besides, the results of the stability test at 40 °C/75% RH for one month also indicates that **Form II** can be slowly converted into **Form I** at 40 °C/75% RH.

VT-PXRD was conducted to further evaluate the relative stability of **Form I** and **Form II** at higher temperature (Fig. 4).

Table 3 The outcome of SDG of a 1 : 1 molar ratio of 5FU and 4HBA from 22 different solvents

Solvent	Dielectric constant (20 °C)[60]	Crystal forms identified by PXRD
n-Heptane	1.92	**Form II**
1,4-Dioxane	2.21 (25 °C)	**Form II**
Benzene	2.28	**Form II**
o-Xylene	2.27	**Form II**
p-Xylene	2.27	**Form II**
m-Xylene	2.37	**Form II**
Chloroform	4.90	**Form II**
Ethyl acetate	6.02	**Form II**
Methyl acetate	6.68 (25 °C)	**Form II**
Tetrahydrofuran	7.58 (25 °C)	**Form II**
Methylene chloride	9.10	**Form II**
sec-Butyl alcohol	15.50	**Form II**
n-Butyl alcohol	17.10	**Form II**
Isopropyl alcohol	18.30 (25 °C)	**Form II**
Butanone	18.51	**Form I** + **Form II**
Acetone	20.70 (25 °C)	**Form I** + **Form II**
Propanol	22.20 (25 °C)	**Form I** + **Form II**
Ethanol	23.80	**Form I** + **Form II**
Methanol	33.10	**Form I**
Acetonitrile	37.50	**Form I**
Ethylene glycol	38.66	**Form I**
Water	78.30	**Form I**

The samples were held for five minutes at each temperature to equilibrate prior to PXRD measurement. The results of the PXRD analysis indicate that **Form I** maintains its crystallinity up to 150 °C, and then it transforms to a mixture of **Form I** and **Form II** in the temperature range of 160–170 °C. Further heating resulted in partial decomposition before complete transformation of **Form I** to **Form II** (Fig. 4). The VT-PXRD data of **Form II** was also obtained, and no evidence of a phase transformation was observed (Fig. S5†). These results normally suggest that the two forms are enantiotropically related. **Form I** is more stable than **Form II** below 150 °C and begins to convert to **Form II** at 160 °C. The thermodynamic transition point lies in the temperature range of 150–160 °C.

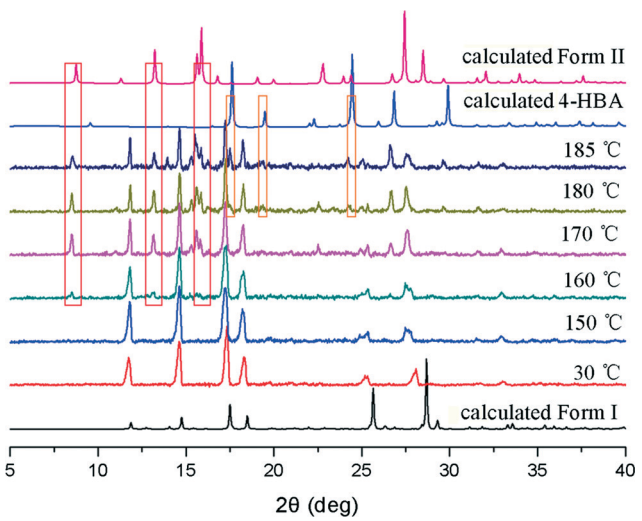

Fig. 4 VT-PXRD analysis of a sample which was initially **Form I** of the 5FU-4HBA co-crystal. A phase transition from **Form I** to **Form II** occurred between 150 and 160 °C.

Conclusions

Two polymorphs of 5FU-4HBA (1 : 1) co-crystals have been isolated by both solid-state grinding and solution crystallization methods. The SDG experiments show a high degree of solvent polarity specificity. High polar solvents tend to favor the generation of **Form I**, while low polar solvents tend to generate **Form II**. Single crystal structure analysis revealed the synthon differences between the molecules of 5FU and 4HBA in two polymorphs, which can also be classified as synthon polymorphs. The crystal structure of **Form I** features an acid–amide heterosynthon, whereas that of **Form II** features an acid–acid homosynthon. A combination of theoretical and experimental methods suggested an enantiotropic relationship between the two polymorphs. **Form I** is more stable at lower temperature while **Form II** is more stable at higher temperature. The thermodynamic transition point for these two enantiotropic forms was found to exist between 150 and 160 °C.

Acknowledgements

This work was financially supported by NSFC (grant no. 21101173, 91127002 and 21331007), NSF of Guangdong Province (S2012030006240), and Guangzhou Pearl River New Star Fund Science and Technology Planning Project (2013J2200054).

References

1 J. Haleblia and W. McCrone, *J. Pharm. Sci.*, 1969, **58**, 911–929.
2 N. Chieng, T. Rades and J. Aaltonen, *J. Pharm. Biomed. Anal.*, 2011, **55**, 618–644.
3 V. S. Minkov, N. A. Tumanov, R. Q. Cabrera and E. V. Boldyreva, *CrystEngComm*, 2010, **12**, 2551–2560.
4 R. M. Vrcelj, J. N. Sherwood, A. R. Kennedy, H. G. Gallagher and T. Gelbrich, *Cryst. Growth Des.*, 2003, **3**, 1027–1032.

5 J. Lu, X. J. Wang, X. Yang and C. B. Ching, *Cryst. Growth Des.*, 2007, **7**, 1590–1598.
6 R. Hilfiker, *Polymorphism: in the Pharmaceutical Industry*, Wiley-VCH, Weinheim, 2006.
7 R. Purohit and P. Venugopalan, *Resonance*, 2009, **14**, 882–893.
8 J. R. Cox, L. A. Ferris and V. R. Thalladi, *Angew. Chem., Int. Ed.*, 2007, **46**, 4333–4336.
9 L. Yu, *CrystEngComm*, 2007, **9**, 847–851.
10 Y. Listiohadi, J. A. Hourigan, R. W. Sleigh and R. J. Steele, *Int. J. Pharm.*, 2008, **359**, 123–134.
11 A. Z. M. Badruddoza, A. I. Toldy, T. A. Hatton and S. A. Khan, *Cryst. Growth Des.*, 2013, **13**, 2455–2461.
12 D. E. Braun, T. Gelbrich, V. Kahlenberg, G. Laus, J. Wieser and U. J. Griesser, *New J. Chem.*, 2008, **32**, 1677–1685.
13 S. R. Vippagunta, H. G. Brittain and D. J. Grant, *Adv. Drug Delivery Rev.*, 2001, **48**, 3–26.
14 N. J. Babu, S. Cherukuvada, R. Thakuria and A. Nangia, *Cryst. Growth Des.*, 2010, **10**, 1979–1989.
15 J. Bernstein, *Polymorphism in Molecular Crystals*, Clarendon, Oxford, 2002.
16 P. M. Bhatt and G. R. Desiraju, *Chem. Commun.*, 2007, 2057–2059.
17 S. P. Thomas, K. Nagarajan and T. N. G. Row, *Chem. Commun.*, 2012, **48**, 10559–10561.
18 S. P. Delaney, E. M. Witko, T. M. Smith and T. M. Korter, *J. Phys. Chem. A*, 2012, **116**, 8051–8057.
19 J. A. Bis, P. Vishweshwar, R. A. Middleton and M. J. Zaworotko, *Cryst. Growth Des.*, 2006, **6**, 1048–1053.
20 T. R. Shattock, P. Vishweshwar, Z. Q. Wang and M. J. Zaworotko, *Cryst. Growth Des.*, 2005, **5**, 2046–2049.
21 S. Skovsgaard and A. D. Bond, *CrystEngComm*, 2009, **11**, 444–453.
22 S. Aitipamula, P. S. Chow and R. B. H. Tan, *CrystEngComm*, 2009, **11**, 889–895.
23 S. Aitipamula, A. B. H. Wong, P. S. Chow and R. B. H. Tan, *CrystEngComm*, 2013, **15**, 5877–5887.
24 T. Friscic and L. R. MacGillivray, *Chem. Commun.*, 2009, 773–775.
25 A. N. Sokolov, D. C. Swenson and L. R. MacGillivray, *Proc. Natl. Acad. Sci. U. S. A.*, 2008, **105**, 1794–1797.
26 A. Mukherjee and G. R. Desiraju, *Chem. Commun.*, 2011, **47**, 4090–4092.
27 A. Mukherjee, P. Grobelny, T. S. Thakur and G. R. Desiraju, *Cryst. Growth Des.*, 2011, **11**, 2637–2653.
28 S. A. Barnett, A. J. Blake and N. R. Champness, *CrystEngComm*, 2003, **5**, 134–136.
29 I. Sarcevica, L. Orola, M. V. Veidis, A. Podjaya and S. Belyakov, *Cryst. Growth Des.*, 2013, **13**, 1082–1090.
30 A. Lemmerer, D. A. Adsmond, C. Esterhuysen and J. Bernstein, *Cryst. Growth Des.*, 2013, **13**, 3935–3952.
31 P. Kaur and T. N. G. Row, *Cryst. Growth Des.*, 2012, **12**, 2744–2747.
32 S. Ghosh, A. Mondal, M. S. R. N. Kiran, U. Ramamurty and C. M. Reddy, *Cryst. Growth Des.*, 2013, **13**, 4435–4441.
33 P. Sanphui, N. J. Babu and A. Nangia, *Cryst. Growth Des.*, 2013, **13**, 2208–2219.
34 G. Bolla, S. Mittapalli and A. Nangia, *CrystEngComm*, 2014, **16**, 24–27.
35 Y. C. Yan, C. E. Hughes, B. M. Kariuki and K. D. M. Harris, *Cryst. Growth Des.*, 2013, **13**, 27–30.
36 P. K. Goswami, R. Thaimattam and A. Ramanan, *Cryst. Growth Des.*, 2013, **13**, 360–366.
37 H. G. Brittain, *Polymorphism in Pharmaceutical Solids*, Marcel Dekker, New York, 1999.
38 A. D. Bond, *Curr. Opin. Solid State Mater. Sci.*, 2009, **13**, 91–97.
39 J. Bernstein, *Cryst. Growth Des.*, 2011, **11**, 632–650.
40 C. Butterhof, K. Bärwinkel, J. Senker and J. Breu, *CrystEngComm*, 2012, **14**, 6744–6749.
41 N. Schultheiss, M. Roe and S. X. M. Boerrigter, *CrystEngComm*, 2011, **13**, 611–619.
42 C. Wales, L. H. Thomas and C. C. Wilson, *CrystEngComm*, 2012, **14**, 7264–7274.
43 J. D. Dunitz, *CrystEngComm*, 2003, **5**, 506–506.
44 J. M. Chen, Z. Z. Wang, C. B. Wu, S. Li and T. B. Lu, *CrystEngComm*, 2012, **14**, 6221–6229.
45 S. Mirza, J. Heinämäki, I. Miroshnyk and J. Yliruusi, *Eur. J. Pharm. Sci.*, 2008, **34**, S16–S17.
46 S. Cherukuvada, N. J. Babu and A. Nangia, *J. Pharm. Sci.*, 2011, **100**, 3233–3244.
47 S. F. Chow, M. Chen, L. Shi, A. H. Chow and C. C. Sun, *Pharm. Res.*, 2012, **29**, 1854–1865.
48 Y. S. Krishnaiah, *J. Bioequivalence Bioavailability*, 2010, **2**, 28–36.
49 Y. Yan, J. M. Chen and T. B. Lu, *CrystEngComm*, 2013, **15**, 6457–6460.
50 J. L. Grem, *Invest. New Drugs*, 2000, **18**, 299–313.
51 B. R. Sreekanth, P. Vishweshwar and K. Vyas, *Chem. Commun.*, 2007, 2375–2377.
52 V. R. Vangala, P. S. Chow and R. B. Tan, *CrystEngComm*, 2011, **13**, 759–762.
53 S. Aitipamula, P. S. Chow and R. B. Tan, *CrystEngComm*, 2012, **14**, 2381–2385.
54 M. C. Etter, *J. Phys. Chem.*, 1991, **95**, 4601–4610.
55 M. S. Pavan, K. D. Prasad and T. N. G. Row, *Chem. Commun.*, 2013, **49**, 7558–7560.
56 M. C. Etter and G. M. Frankenbach, *Chem. Mater.*, 1989, **1**, 10–12.
57 V. R. Pedireddi, W. Jones, A. P. Chorlton and R. Docherty, *Chem. Commun.*, 1996, 987–988.
58 D. R. Weyna, T. Shattock, P. Vishweshwar and M. J. Zaworotko, *Cryst. Growth Des.*, 2009, **9**, 1106–1123.
59 S. Karki, T. Friscic, W. Jones and W. D. S. Motherwell, *Mol. Pharmaceutics*, 2007, **4**, 347–354.
60 L. L. Chen, *Solvents Handbook*, Chemical Industry Press, Beijing, 2007.
61 A. V. Trask, W. S. Motherwell and W. Jones, *Chem. Commun.*, 2004, 890–891.
62 M. D. Eddleston, S. Sivachelvam and W. Jones, *CrystEngComm*, 2013, **15**, 175–181.
63 S. Aitipamula, P. S. Chow and R. Tan, *CrystEngComm*, 2010, **12**, 3691–3697.
64 S. Aitipamula, A. B. Wong, P. S. Chow and R. B. Tan, *CrystEngComm*, 2012, **14**, 8193–8198.
65 A. Burger and R. Ramberger, *Microchim. Acta*, 1979, **72**, 259–271.

